Measurement fusion method for indoor localization of a walking robot

Benedykt Jaworski, Dominik Bilicki, Dominik Belter

Institute of Control and Information Engineering, Poznań University of Technology

Abstract: The article presents visual localization system for walking robots. The method uses two independent visual procedures to determine position and orientation of the robot's body: Parallel Tracking and Mapping (PTAM) and the procedure which returns position of the camera in relation to the known marker. The heuristic-based data fusion method is proposed. The method takes into account properties of both modules to estimate real position of the robot. The properties of the method are presented using ground truth data from experiment on the robotic arm.

Keywords: visual localization system, data fusion, mobile robot

1. Introduction

1.1. Problem statement

Localization of a robot is a fundamental problem in robotics. Without information about position, the robot cannot efficiently move in the environment. The robot can only avoid obstacles by using simple reactive behavior. To reach a distant goal the robot should plan its motion using knowledge about its position and configuration of the environment. It is efficient way to execute the autonomous mission of a mobile robot.

In our research we use six-legged walking robot (fig. 1). The robot can walk in rough and unstructured environment [2]. The orientation of the robot's body changes constantly. It is necessary to estimate full state of the robot (position and orientation). We can use the initial guess about position and orientation of the robot by taking into account control signal. However, the error between real and estimated position of the robot quickly increases because of slippages. The problem of legged robot localization is related to recovering the 6D motion of the hand-held camera. In contrast to differential-drive mobile robot, kinematic model of the walking robot is not useful for localization.

The Messor robot used in this research can carry less than 0.5 kg. Thus, we cannot use heavy sensors like SICK Laser Range Finder to built a map and localize the robot [4]. We are looking for localization system which works properly indoors in previously prepared environment. Such a system is required to verify motion planning and control algorithms for mobile robots in laboratory. Thus, GPS-based localization systems [13] are not acceptable. In this paper we present results of our search for localization system which is light, fast, reliable, inexpensive, and which can be used indoors on the real walking robot.

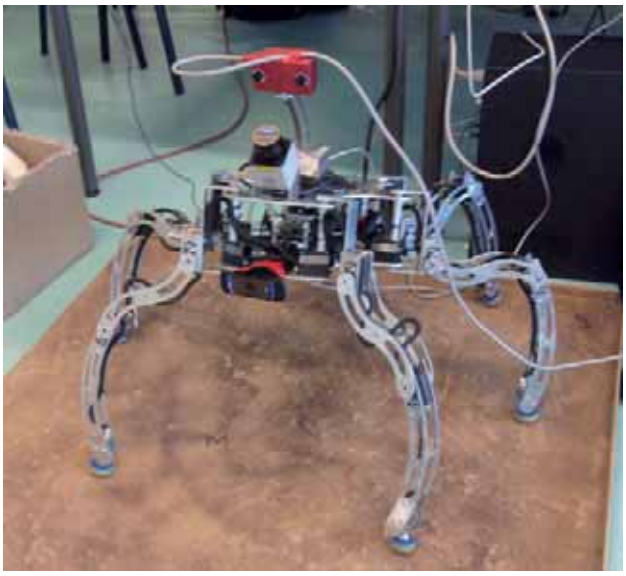

Fig. 1. Messor robot
Rys. 1. Robot Messor

1.2. Related work

Many solutions to localization problem were proposed. Most of them are focused on Simultaneous Localization and Mapping (SLAM). As a core of this method the Kalman Filtering can be used [15]. In this approach, the motion model is used in prediction phase. Then the observation model, which uses exteroceptive sensors, updates the previous *a priori* estimation of the robot's state. Recently, the graph-based SLAM with optimization and loop closure detection becomes more popular [12].

SLAM framework can be very efficient for long-life experiments in large areas [16]. In our case the precision is more important than the capability to operate in large environment. In contrary to SLAM, the PTAM (Parallel Tracking and Mapping) algorithm was proposed [8]. In this approach feature tracking plays important role. As a result high precision localization system for small workspaces was obtained. Also visual odometry allows to obtain precise information about frame to frame transformation by using template matching [3]. Similarly, the geometrical features obtained by using laser range finder can be matched to create estimation of the robot's pose as well as model of the environment [14].

There are also many localization systems dedicated for indoor experiments. One of them is StarGazer localization

system [5]. The robot observes known landmarks located on the ceiling. The robot uses infrared projector to increase robustness and detect a passive marker in various light conditions. The reflected infrared rays are easily detected by the camera. According to the acquired image, the robot calculates its position and orientation. The application of this system is limited by price and size of the sensor.

For indoor localization also beacon systems are used [10]. The concept is based on distance or angle measurements to stationary beacons. The triangulation is used to determine position of the robot. It is mainly used for the 2D localization problem.

Another possibility to recover the full state of the robot is to use motion capture system. Several cameras observe known markers which are attached to the robot's body. Such systems are successfully used in systems used for recording fast human motion [17] as well as for film-making and computer games. It was also used to localize walking robot during indoor experiments [6]. Although the precision and speed of the system is high, it is expensive.

In our approach we decided to integrate results from two localization systems. The first one is PTAM, which is very precise for small workspaces, but the localization error tends to accumulate. Therefore, we decided to use system which determines absolute position of camera in relation to known marker. Because robot's legs might obscure the marker, we decided to locate the marker on the wall and camera on robot's board. In this case we can use large markers to obtain high precision and big workspace. Obviously it is not possible if the marker is located on the robot. As a marker we use 0.8 m × 0.6 m checkerboard.

2. Localization system

2.1. Kinematic structure

The localization system combines data from two independent modules. We use complementary approach. The final system combines results from two independent modules and resolves incompleteness of sensory data. Both modules return information about 6D pose of the camera. Each module uses its own independent camera. The PTAM module returns reliable and precise information about camera pose only in feature-rich environment. For that reason the camera of the PTAM module is tilted down [1]. During walking the robot observes rough and irregular terrain which is feature reach. The camera of the checkerboard module is mounted horizontally to easily observe and detect the checkerboard marker.

The PTAM module returns transformation $\mathbf{P}$ from PTAM fixed base coordinate system O_{BP} to the current pose of the camera O'_{P} (fig. 2). The initial position of the PTAM camera is O_{P} described by the transformation $\mathbf{P}_{\mathrm{P}}$. We use (1) to determine the transformation $\mathbf{O}'_{\mathrm{P}}$ from the initial position of the PTAM camera O_{P} to the current position O'_{P}:

$$\mathbf{P}_0 \quad = \quad \mathbf{P}_{\mathrm{P}}^{-1} \cdot \mathbf{P} \ , \tag{1}$$

Similarly, the checkerboard module returns transformation $\mathbf{S}$ from checkerboard fixed base coordinate system O_{BS} to the current pose of the camera O'_{S} (fig. 2). The initial position of the checkerboard camera is O_{S}, described

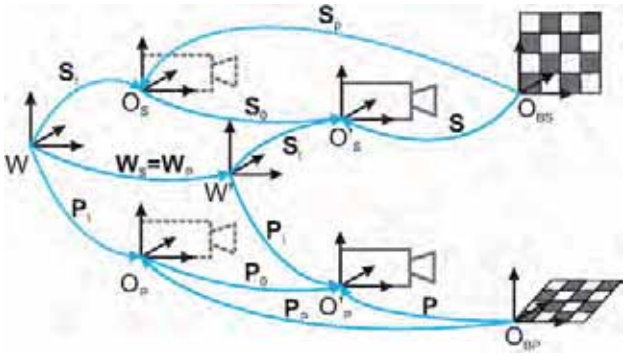

Fig. 2. Kinematic configuration of the sensory system
Rys. 2. Konfiguracja kinematyczna systemu lokalizacji

by the transformation $\mathbf{S}_{\mathrm{P}}$. We use (2) to determine the transformation $\mathbf{O}'_{\mathrm{P}}$ from the initial position of the PTAM camera O_{P} to the current position O'_P:

$$\mathbf{S}_0 \quad = \quad \mathbf{S}_{\mathrm{P}}^{-1} \cdot \mathbf{S} \ , \tag{2}$$

In order to properly combine results from both modules, we determine the position of the robot in the common coordinate system W' (W' is attached to the chassis which keeps two cameras together). Then, we determine the transformation from the initial position of the common coordinate system W to the current position of the common coordinate system W'. The transformation $\mathbf{W}_{\mathrm{S}}$ (3) is computed using results from checkerboard system:

$$\mathbf{W}_{\mathrm{S}} \quad = \quad \mathbf{S}_{\mathrm{t}} \cdot \mathbf{S}_0 \cdot \mathbf{S}_{\mathrm{t}}^{-1} \ , \tag{3}$$

where $\mathbf{S}_{\mathrm{t}}$ is a fixed transformation from common coordinate system W to checkerboard camera coordinate system O_{S}.

Similar computation is used for transformation $\mathbf{W}_{\mathrm{P}}$ (4) which determines the position of the common coordinate system W' according to the PTAM measurements:

$$\mathbf{W}_{\mathrm{P}} \quad = \quad \mathbf{P}_{\mathrm{t}} \cdot \mathbf{P}_0 \cdot \mathbf{P}_{\mathrm{t}}^{-1} \ , \tag{4}$$

where $\mathbf{P}_{\mathrm{t}}$ is a fixed transformation from common coordinate system W to PTAM camera coordinate system O_{P}.

Finally, we compute the position of the common coordinate system using eqs. (5) and (6):

$$\mathbf{W}_{\mathrm{S}} \quad = \quad \mathbf{S}_{\mathrm{t}} \cdot \mathbf{S}_{\mathrm{P}}^{-1} \cdot \mathbf{S} \cdot \mathbf{S}_{\mathrm{t}}^{-1} \ , \tag{5}$$

$$\mathbf{W}_{\mathrm{P}} \quad = \quad \mathbf{P}_{\mathrm{t}} \cdot \mathbf{P}_{\mathrm{P}}^{-1} \cdot \mathbf{P} \cdot \mathbf{P}_{\mathrm{t}}^{-1} \ . \tag{6}$$

In ideal conditions without measurement error, $\mathbf{W}_{\mathrm{S}}$ should be equal to $\mathbf{W}_{\mathrm{P}}$.

2.2. PTAM module calibration

Although PTAM module returns information about position of the camera, the scale varies strongly. The scale depends on images chosen for initialization. The robot requires metric scale to use the estimated position for motion planning. To recover metric scale the robot performs additional calibration experiment. The robot moves its body along each axis of the global coordinate system W. The distance along each axis is set to 10 cm. The robot computes

the distance along each axis measured in PTAM coordinate system O_{BP}. When the robot translates along x axis it computes vector $\mathbf{d}x$:

$$\begin{aligned} dx_x &= x_{x\mathrm{p}} - x_{x\mathrm{n}} \\ dy_x &= y_{x\mathrm{p}} - y_{x\mathrm{n}} \\ dz_x &= z_{x\mathrm{p}} - z_{x\mathrm{n}} \end{aligned}, \tag{7}$$

where $x_{x\mathrm{p}}$ is an initial x position of the PTAM camera and $x_{x\mathrm{n}}$ is the position of the camera at the end of the motion. The same convention is used for y and z axes and the vectors $\mathbf{d}y$ and $\mathbf{d}z$ are computed for the transition along y and z axes. Then, the matrix **Tmp** is computed:

$$\begin{bmatrix} \frac{dx_x}{\sqrt{dx_x^2+dy_x^2+dz_x^2}} & \frac{dx_y}{\sqrt{dx_y^2+dy_y^2+dz_y^2}} & \frac{dx_z}{\sqrt{dx_z^2+dy_z^2+dz_z^2}} & \mathbf{P}_{\mathrm{p}}(1,4) \\ \frac{dy_x}{\sqrt{dx_x^2+dy_x^2+dz_x^2}} & \frac{dy_y}{\sqrt{dx_y^2+dy_y^2+dz_y^2}} & \frac{dy_z}{\sqrt{dx_z^2+dy_z^2+dz_z^2}} & \mathbf{P}_{\mathrm{p}}(2,4) \\ \frac{dz_x}{\sqrt{dx_x^2+dy_x^2+dz_x^2}} & \frac{dz_y}{\sqrt{dx_y^2+dy_y^2+dz_y^2}} & \frac{dz_z}{\sqrt{dx_z^2+dy_z^2+dz_z^2}} & \mathbf{P}_{\mathrm{p}}(3,4) \\ 0 & 0 & 0 & 1 \end{bmatrix}, \tag{8}$$

where $\mathbf{P}_{\mathrm{p}}(i,j)$ are i-th and j-th elements of the $\mathbf{P}_{\mathrm{p}}$ matrix (fig. 2).

To recover metric scale the vector **scale** is computed:

$$\mathbf{scale} = [x_{\mathrm{scale}}, y_{\mathrm{scale}}, z_{\mathrm{scale}}, 1]^T, \tag{9}$$

where $x_{\mathrm{scale}} = \frac{0.1}{\sqrt{dx_x^2+dy_x^2+dz_x^2}}$, $y_{\mathrm{scale}} = \frac{0.1}{\sqrt{dx_y^2+dy_y^2+dz_y^2}}$ and $z_{\mathrm{scale}} = \frac{0.1}{\sqrt{dx_z^2+dy_z^2+dz_z^2}}$.

The vector **scale** is used to scale transitions obtained by using PTAM module. Results are in metric scale. The matrix **Tmp** is used to rotate the O_{BP} coordinate system. Using the transformation **Tmp** the initial positions of the coordinate systems O_P and O_{BP} have the same position and orientation. Finally, the PTAM module returns transformation:

$$\mathbf{P} = \mathbf{Tmp}^{-1} \cdot \mathbf{P}_{\mathrm{PTAM}}. \tag{10}$$

Then, the metric scale is recovered using element-by-element product of the last column of the $\mathbf{P}$ and vector **scale**.

2.3. Measurement fusion

According to (5) and (6) the PTAM and checkerboard modules return information about position of the $\mathbf{W}'$ coordination system determined in the initial position of the common coordinate system $\mathbf{W}$. The values returned by PTAM and checkerboard module are not always the same. Because of the sensor noise and properties of the position estimation methods the returned values are different. To compute final position of the camera system we use heuristic approach for measurement fusion.

The most popular method for measurements fusion is the Kalman filter. Various modifications to the Kalman filtering can be used to obtain general framework for integration multi-system measurements [9]. The Kalman filter stores information about past state of the system. The sensor failure might cause significant measurement error [9]. For multi-sensor data fusion and fault detection a Support Vector Machine and adaptive neuro-fuzzy inference system (ANFIS) can be used [7]. It was also presented that the heuristic system, which takes into account the expert knowledge about phenomena, can outperform Kalman filtering [11]. The fuzzy logic is proposed as a better alternative to Kalman filter to combine odometry with optical gyroscope.

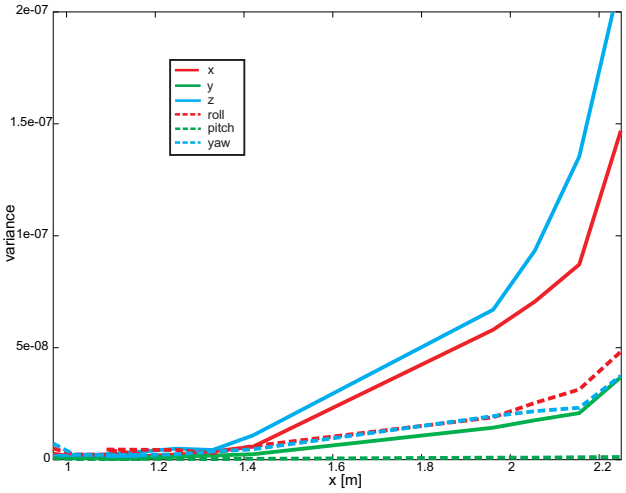

Fig. 3. Relation between distance and variance for the checkerboard-camera system

Rys. 3. Zależność pomiędzy odległością a wariancją dla układu kamera-szachownica

The integration procedure in our localization system computes weighted mean value of both measurements. Weights are inversely proportional to variance of both systems. The PTAM module has three constant variances. The variance depends on the information about tracking quality which is returned by PTAM algorithm [8]. Three levels of certainty are distinguished: good tracking (the smallest variance), poor quality and lost tracking (the variance is ∞).

In the checkerboard module the quality of measurements decreases when the distance to the checkerboard increases. Despite the fact that the marker is big, when the distance is large, image resolution and size of the pixel play important role. We performed verification experiment to find the relation between distance and the variance of measurements for checkerboard module (fig. 3). The results of the experiment show that the relation between distance to the checkerboard and variance is exponential. We approximated this relation using third degree polynomial.

The variance matrices for PTAM and checkerboard measurements are diagonal. We assume that 6D coordinates are not correlated. Only diagonal elements of 6×6 variance matrices are not equal to zero.

Taking into account the variance matrices and the results obtained from PTAM and checkerboard modules, the final position is computed using the weighted mean value (note that we use inverse of the variance as a weighting factor):

$$\mathbf{x} = (\mathbf{S}_{\mathrm{VAR}}^{-1} + \mathbf{P}_{\mathrm{VAR}}^{-1})^{-1} \cdot (\mathbf{S}_{\mathrm{VAR}}^{-1} \cdot \mathbf{x}_S + \mathbf{P}_{\mathrm{VAR}}^{-1} \cdot \mathbf{x}_P), \tag{11}$$

where $\mathbf{S}_{\mathrm{VAR}}$ and $\mathbf{P}_{\mathrm{VAR}}$ are variance matrices for checkerboard and PTAM, respectively. Coordinates with S index are obtained using Checkerboard and with P are obtained using PTAM.

Finally, we use (12) to compute the position estimates:

Fig. 4. Testbed for experiment with KUKA robotic arm
Rys. 4. Stanowisko do eksperymentu na manipulatorze przemysłowym KUKA

$$\begin{bmatrix} x \\ y \\ z \\ \alpha \\ \beta \\ \gamma \end{bmatrix} = \begin{bmatrix} x_{\mathrm{S}} \\ y_{\mathrm{S}} \\ z_{\mathrm{S}} \\ \alpha_{\mathrm{S}} \\ \beta_{\mathrm{S}} \\ \gamma_{\mathrm{S}} \end{bmatrix} + \mathbf{K} \cdot \left(\begin{bmatrix} x_{\mathrm{P}} \\ y_{\mathrm{P}} \\ z_{\mathrm{P}} \\ \alpha_{\mathrm{P}} \\ \beta_{\mathrm{P}} \\ \gamma_{\mathrm{P}} \end{bmatrix} - \begin{bmatrix} x_{\mathrm{S}} \\ y_{\mathrm{S}} \\ z_{\mathrm{S}} \\ \alpha_{\mathrm{S}} \\ \beta_{\mathrm{S}} \\ \gamma_{\mathrm{S}} \end{bmatrix} \right), \quad (12)$$

where α, β and γ are rotations around x, y, z axes (roll, pitch, yaw angles in RPY Euler angles notation).

The matrix $\mathbf{K}$ is computed according to the equation:

$$\mathbf{K} = \mathbf{S}_{\mathrm{VAR}} \cdot \left(\mathbf{S}_{\mathrm{VAR}} + \mathbf{P}_{\mathrm{VAR}}\right)^{-1}. \quad (13)$$

3. Results

3.1. System verification

Verification of the measurement fusion system was performed using KUKA manipulator robotic arm. The experimental set is presented in fig. 4. Two cameras are attached to the end effector of the robot. The camera of the checkerboard system is mounted horizontally. It allows to detect the checkerboard marker which is located on the vertical wall. The camera of the PTAM module is tilted down. It observes the rough terrain mockup (feature-reach environment).

At the beginning of the experiment the PTAM module is calibrated to recover metrical scale. Then, the end effector moves in the workspace. The reference motion of the end effector is assumed as ground truth. We save the path returned by PTAM and checkerboard module and the final path. The results are shown in fig. 5.

At the beginning of the experiment the cameras are moved towards the checkerboard (along y axis) (fig. 5 A). The motion along x and z axes is parallel to surface of the checkerboard marker. In the fig. 5 B, C and D one can see the results of the localization algorithms and final measurements fusion for each axis of the global coordinate system W. The measurements from both modules differ. The final position estimation is a combination of two initial PTAM and checkerboard estimations.

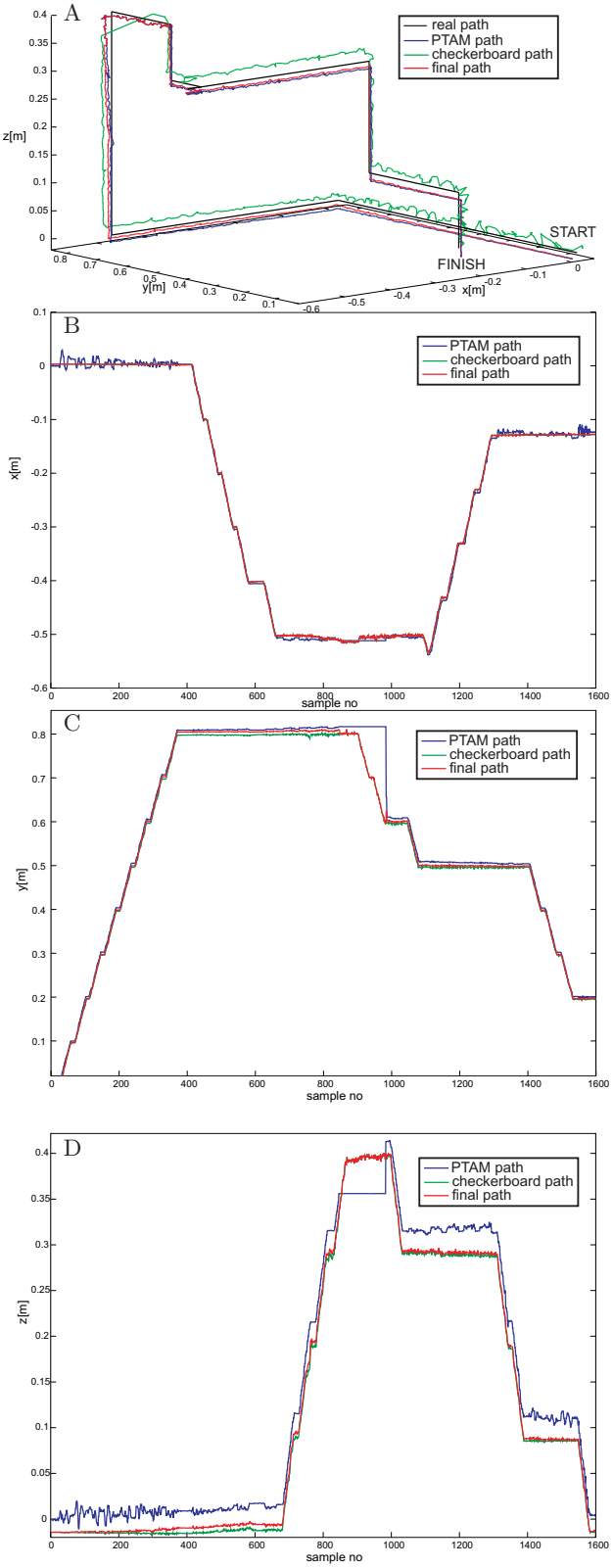

Fig. 5. Results of the experiment on the KUKA robotic arm
Rys. 5. Wyniki eksperymentu przeprowadzonego na manipulatorze przemysłowym KUKA

It can be also seen that between 800 and 1000 sample, the final estimated position is equal to the position given by the PTAM module. The checkerboard camera lost the marker. In this case the values on diagonal of matrix $\mathbf{S}_{\mathrm{VAR}}$ are set to ∞. In this case the system ignores data

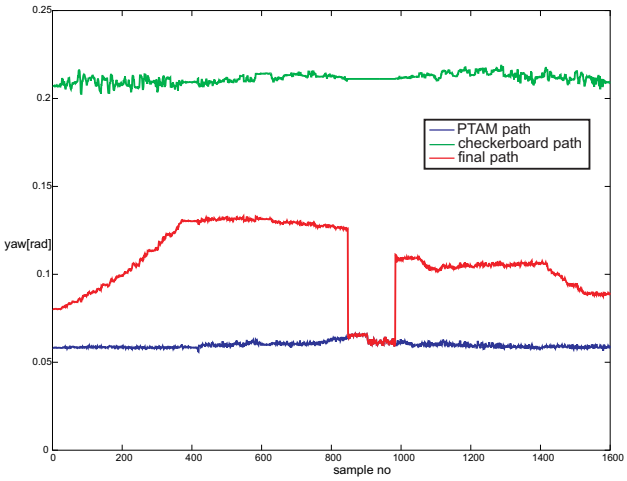

Fig. 6. Influence of change of the variance matrix on the ultimate result of measurements
Rys. 6. Wpływ zmiany macierzy kowariancji na ostateczny wynik pomiaru

from the checkerboard module and uses data only from the PTAM module. During all experiments, the error does not exceed 2 cm.

The properties of the measurements fusion strategy can be seen in fig. 6. In fig. 6 the measured yaw angle is presented. The real value of the yaw angle during the experiment was constant and set to zero. The values measured by PTAM and checkerboard modules are constant but not equal zero. A constant offset can be observed. It suggests that extrinsic parameters of the cameras (transformations $\mathbf{S}_t$ and $\mathbf{P}_t$) are not well calibrated.

At the beginning of the experiment presented in fig. 6 the weights connected to the PTAM module are bigger (the variance of the PTAM measurements is smaller). When the end effector with cameras approaches checkerboard marker the measurements variance of the checkerboard module decreases. The checkerboard module returns more reliable data. The system takes into account these properties of the measurement system during computation of the final pose estimation according to (12). The weights of the checkerboard measurements increase and the final estimation of the yaw angle (fig. 6) becomes closer to the results obtained using the checkerboard module. Again, between 800 and 1000 sample one can see the situation when the checkerboard camera lost the tracked target and the final estimation was the same as the estimation from the PTAM module.

Additional experiment was performed to show the properties of the localization system when the cameras are rotated. Again, the constant offset can be observed. The reference pitch angle (rotation around y axis) was modified by 10° at each step during the experiment. The system properly measures the behavior of the camera and the measurement error does not exceed 4°. It can be used on the real robot. However, the inertial measurement units, that is, XSense MTi, have better accuracy.

Another property of the system can be seen in fig. 7. At the end of the experiment the angle measured by checkerboard decreases whilst the angle measured by PTAM increases. The real angle value was increasing. The checkerboard module returns erroneous values, because the marker used is rotational invariant (for pitch angle 180° and 0° the image of the checkerboard is the same). In the future we are going to add color to the single field of the checkerboard to deal with ambiguity and to determine the orientation of the camera.

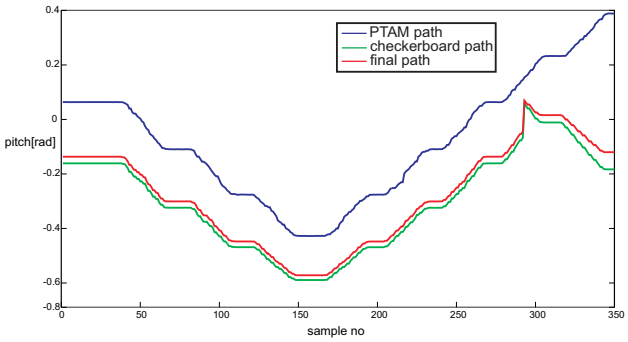

Fig. 7. Measured *pitch* angle during experiment with the KUKA robot
Rys. 7. Zmierzony kąt *pitch* podczas eksperymentu na robocie KUKA

4. Conclusions and future work

The article presents the measurement fusion strategy for indoor localization system. The data from PTAM and the checkerboard module are combined to obtain more reliable measurements. The fusion method takes into account the properties of both methods. The variance is used as a weighting factor. When the cameras are close to the checkerboard the role of the PTAM module decreases. Similarly, if the observed scene is not feature-rich the certainty of the PTAM measurements decreases and the system relies mainly on measurements from the checkerboard module.

The obtained results can be used to localize a 6-dof mobile robot indoors. The system is useful for walking and flying robots, where data from odometry are not reliable. The system can estimate 6-dof pose of the robot. However, the data about orientation are less reliable. If it is possible, the system can be supported by high-quality Attitude and Heading Reference System (AHRS).

The proposed measurement fusion can be used as an alternative to expensive motion capture systems. The system is inexpensive – only two USB cameras are required. Moreover, the proposed system is fast and can be used to estimate position of the robot 15 times per second.

In the future we are going to use an AHRS system as additional input to the system to obtain more reliable information about the inclination of the robot's platform.

Acknowledgement

This work was supported by the National Science Centre of Republic of Poland, grant no. 2011/01/N/ST7/02080.

References

1. Belter D., Skrzypczyński P., *Precise self-localization of a walking robot on rough terrain using PTAM*, [in:] A. Azad et al. (Eds.), *Adaptive Mobile Robotics*, World Scientific, Singapore 2012, 89–96.

2. Belter D., Skrzypczyński P., *Rough terrain mapping and classification for foothold selection in a walking robot*, "Journal of Field Robotics", Vol. 28, No. 4, 2011, 497–528.
3. Gonzalez R., Rodriguez F., Guzman J., Pradalier C., Siegwart R., *Combined Visual Odometry and Visual Compass for Off-Road Mobile Robots Localization*, "Robotica", Vol. 30, No. 6, 2011, 1–14.
4. Grisetti G., Stachniss C., Burgard W., *Improving Grid-based SLAM with Rao-Blackwellized Particle Filters by Adaptive Proposals and Selective Resampling*, [in:] Proc. of the IEEE International Conference on Robotics and Automation (ICRA), Barcelona, Spain, 2005, 2432–2437.
5. [www.hagisonic.com] – Leading company of advanced sensors – Hagisonic (January 2013).
6. Kalakrishnan M., Buchli J., Pastor P., Mistry M., Schaal S., *Fast, robust quadruped locomotion over challenging terrain*, IEEE International Conference on Robotics and Automation (ICRA), 2010, 2665–2670.
7. Salahshoora K., Kordestanib M., Khoshrob M.S., *Fault detection and diagnosis of an industrial steam turbine using fusion of SVM (support vector machine) and ANFIS (adaptive neuro-fuzzy inference system) classifiers*, 3rd International Conference on Sustainable Energy and Environmental Protection (SEEP 2009), Vol. 35, No. 12, December 2010, 5472–5482.
8. Klein G., Murray D.W., *Parallel Tracking and Mapping for Small AR Workspaces*, [in:] Proc. of ISMAR, 2007, 225–234.
9. Lee T.G., *Centralized Kalman Filter with Adaptive Measurement Fusion: its Application to a GPS/SDINS Integration System with an Additional Sensor*, "International Journal of Control, Automation, and Systems", Vol. 1, No. 4, 2003, 444–542.
10. Navarro-Serment L.E., Paredis C.J.J., Khosla P.K., *A Beacon System for the Localization of Distributed Robotic Teams*, [in:] Proceedings of the International Conference on Field and Service Robotics, 1999, 232–237.
11. Ojeda L., Borenstein J., *FLEXnav: Fuzzy Logic Expert Rule-based Position Estimation for Mobile Robots on Rugged Terrain*, [in:] Proceedings of the IEEE International Conference on Robotics and Automation, Washington, USA, 2002, 317–322.
12. Pinies P., Paz L.M., Galvez-Lopez D., Tardos J.D., *CI-Graph SLAM for 3D Reconstruction of Large and Complex Environments using a Multicamera System*, "International Journal of Field Robotics", Vol. 27, No. 5, 2010, 561–586.
13. Reina G., Vargas A., Nagatani K., Yoshida K., *Adaptive Kalman Filtering for GPS-based Mobile Robot Localization*, IEEE International Workshop on Safety, Security and Rescue Robotics, 2007, 1–6.
14. Skrzypczyński P., *Laser scan matching for self-localization of a walking robot in man-made environments*, [in:] Bidaud P. et al. (Eds.), *Field Robotics: Proceedings of the 14th International Conference on Climbing and Walking Robots and the Support Technologies for Mobile Machines*, World Scientific, 2011, 825–832.
15. Skrzypczyński P., *Simultaneous localization and mapping: A feature-based probabilistic approach*, "International Journal of Applied Mathematics and Computer Science", Vol. 19, No. 4, 2009, 575–588.
16. Strasdat H., Montiel J.M.M., Davison A.J., *Scale Drift-Aware Large Scale Monocular SLAM*, Robotics: Science and Systems, 2010.
17. Suleiman W., Yoshida E., Kanehiro F., Laumond J-P, Monin A., *On human motion imitation by humanoid robot*, IEEE International Conference on Robotics and Automation, 2008, 2697–2704.

Integracja danych pomiarowych w systemie lokalizacji robota kroczącego

Streszczenie: Artykuł przedstawia wizyjny system lokalizacji robota kroczącego. Przedstawiono wykorzystanie algorytmu PTAM oraz metody określającej położenie kamery względem znacznika do określenia położenia robota. Przedstawiono metodę fuzji danych z obu systemów pomiarowych. Proponowana metoda jest alternatywą dla droższych systemów 'motion capture' wykorzystywanych do weryfikacji eksperymentalnej wewnątrz laboratorium.

Słowa kluczowe: lokalizacja robota mobilnego, fuzja danych, system wizyjny

Benedykt Jaworski

Since 2010 studies control and robotics at the Poznań University of Technology, with special interest in programming techniques, artificial intelligence and sensory systems. He is a member of CybAir scientific group.
e-mail: b.jaworski@kofeina.net

Dominik Bilicki

Studies control and robotics at the Poznań University of Technology, with special interest in modeling and sensory systems. He is a member of CybAir scientific group.
e-mail: dkbilicki@gmail.com

Dominik Belter, PhD

Received the MSc degree in control engineering and robotics from the Poznań University of Technology in 2007. Since then he had been working as a research assistant at the Institute of Control and Information Engineering of the same university. In 2012 he finished his PhD in robotics. Since 2012 he has been working as an assistant professor at the PUT. He is a member of IEEE Robotics and Automation Society. His research interests include: control of walking robots, machine learning, and soft computing.
e-mail: dominik.belter@put.poznan.pl